

Simulation of vibrations of Ting Kau Bridge due to vehicular loading from measurements

F.T.K. Au^{*1}, P. Lou^{1,2}, J. Li^{1,3}, R.J. Jiang^{1,4}, J. Zhang¹, C.C.Y. Leung¹, P.K.K. Lee¹,
J.H. Lee^{1,5}, K.Y. Wong⁶ and H.Y. Chan⁶

¹Department of Civil Engineering, The University of Hong Kong, Pokfulam Road, Hong Kong, China

²School of Civil Engineering, Central South University, 22 Shao-shan-nan Road, Changsha, Hunan, China

³Department of Civil Engineering, South China University of Technology, Guangzhou, China

⁴School of Civil Engineering, Shandong University, Jinan, Shandong, China

⁵Department of Infrastructure Civil Engineering, Chonbuk National University, Korea

⁶Bridges and Structures Division, Highways Department, The Government of the Hong Kong Special Administrative Region, China

(Received December 15, 2010, Revised July 11, 2011, Accepted August 18, 2011)

Abstract. The Ting Kau Bridge in Hong Kong is a cable-stayed bridge comprising two main spans and two side spans. The bridge deck is supported by three towers, an end pier and an abutment. Each of the three towers consists of a single reinforced concrete mast strengthened by transverse cables and struts. The bridge deck is supported by four inclined planes of cables emanating from anchorages at the tower tops. In view of the heavy traffic on the bridge, and threats from typhoons and earthquakes originated in areas nearby, the dynamic behaviour of long-span cable-supported bridges in the region is always an important consideration in their design. Baseline finite element models of various levels of sophistication have been built not only to match the bridge geometry and cable forces specified on the as-constructed drawings but also to be calibrated using the vibration measurement data captured by the Wind and Structural Health Monitoring System. This paper further describes the analysis of axle loading data, as well as the generation of random axle loads and simulation of vibrations of the bridge using the finite element models. Various factors affecting the vehicular loading on the bridge will also be examined.

Keywords: cable-stayed bridge; dynamic response; finite element; numerical simulation; random vibration; vehicular axle load

1. Introduction

Various researchers have investigated the dynamic behaviour of vehicle-bridge interaction taking into account the random rail or road irregularities. For example, Wiriyachai *et al.* (1982) used a 4-axle train model to study the impact effects on simply supported truss railway bridges with random rail irregularities. Coussy *et al.* (1989) carried out a theoretical study on the effects of random surface irregularities upon the dynamic response of bridges under suspended moving loads. Wang and Huang (1992) employed a single 3-axle moving truck model of 7 degrees-of-freedom (DOFs)

*Corresponding author, Professor, E-mail: francis.au@hku.hk

to investigate the dynamic response of a cable-stayed highway bridge taking into account the random road surface roughness. Yang *et al.* (1995) carried out the dynamic analysis of a cable-stayed bridge with a 60 m main span using a 6-axle vehicle model considering the random rail irregularities. Kawatani *et al.* (1998) adopted a 3-axle truck model to study the non-stationary random vibration of a simple girder-bridge. Au *et al.* (2002) studied the vibration of cable-stayed bridges considering random rail irregularities under moving railway trains. Wu and Yang (2003) investigated the steady-state response and riding comfort of a train moving over a series of simply supported railway bridges taking into account random rail irregularities. Law and Zhu (2005) studied the dynamic behaviour of a multi-span non-uniform bridge considering the effect of interaction between the structure, the road surface roughness and also the vehicle.

Actually in a vehicle-bridge interaction system, besides the random irregularities of rail or road surface, the vehicle load is also random. For example, Chang *et al.* (2009) estimated the dynamic response of a system excited by a vehicle with random vehicle mass moving at random velocity. However, in most of the previous work with random surface irregularities, the vehicle load was considered as constant. There are various methods of studying vehicle-bridge interaction of which finite element method is extensively used (Song and Choi 2002, Yang 2005, Kwasniewski 2006, Lee 2006, Jo *et al.* 2008, Song and Fujino 2008, Li 2010). This paper reports some of the findings in the development of bridge rating system of Ting Kau Bridge, which are related to vehicular loading. One of the objectives is to develop a procedure for generating the random vehicular axle loading based on the measurements, while the other is to study the resulting dynamic response of the bridge. Compared with the weight of the bridge, the vehicular loading is very small. Therefore in the present study, the vehicular loading is modelled as forces while the road surface irregularities are not considered. In addition, the effects of various parameters on the vehicular loading, including axle spacing, number of axles in each vehicle, distance between vehicles, etc. will be examined.

2. Finite element model of Ting Kau Bridge

Ting Kau Bridge (TKB) is a key component of the transportation network in Hong Kong. It is a four-span cable-stayed bridge carrying a six-lane dual carriageway. The overall span length is 1,177 m with the span configuration of 127 m + 448 m + 475 m + 127 m (The University of Hong Kong, 2000). The northbound (Ting Kau bound) and southbound (Tsing Yi bound) carriageways are separated by a gap within which the towers are located. The suspended deck of the bridge is supported by stay cables which are in turn anchored to three single-leg concrete towers. The deck carrying each carriageway is formed by composite construction with concrete slabs resting on transverse steel girders that are in turn supported by two longitudinal steel main girders. One out of three transverse girders of a carriageway is extended through the gap and connected to the other deck. Fig. 1 shows the plan and elevation of TKB. More details have been given by Au *et al.* (2003). For convenience, the four main girders are labelled as the first, second, third and fourth main girders from West to East.

To account for the distribution of stiffness and mass in the present analyses, the bridge deck is simulated by a grillage model with the grillage members aligned with the longitudinal and transverse girders. The sectional properties of the beam element simulating each grillage member are calculated from the composite section comprising concrete slab and steel girder on the basis of modular ratio, which is the ratio of the modulus of elasticity of steel to that of concrete. An

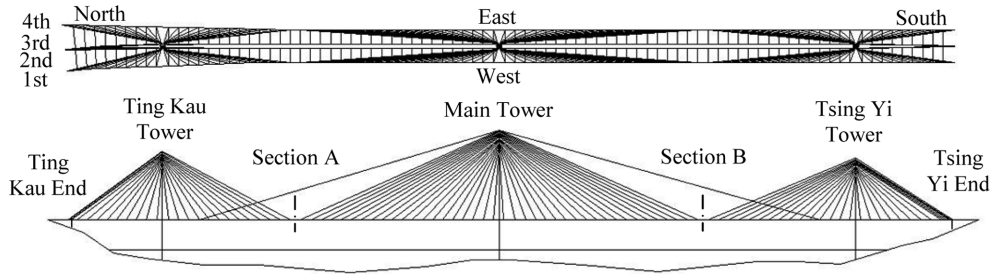


Fig. 1 Schematic plan and elevation of Ting Kau Bridge

extensive study on the shear lag effect has been performed to determine the effective width of slab to be considered when calculating sectional properties (Au *et al.* 2007). The stay cables are simulated by link elements taking into account the prevalent cable forces under permanent loading with the sag effect modelled by the Ernst modulus. To develop an accurate model, it should be calibrated to satisfy the baseline scheme so that the deck profile of the bridge under permanent loading agrees reasonably well with the design profile. The initial cable forces of the baseline model can be determined using the flexibility method as follows

$$\{T_j\} = -[f_{ij}]^{-1} \{\Delta_i\} \tag{1}$$

where $[f_{ij}]$ is the flexibility matrix, $\{T_j\}$ is the cable force vector that contains the tensile forces in all cables, $\{\Delta_i\}$ is the initial displacement vector containing the displacements at all control points of the bridge under permanent loading only, and subscripts i and j denote the i^{th} control point and j^{th} cable considered in the calibration respectively. If necessary, the cable forces can be further adjusted by iteration to satisfy, for example, various allowable stress limits as well.

The finite element modelling and analyses described in this paper are performed using ANSYS Multiphysics 10 University Edition. The complete grid model of TKB consists of 5,594 BEAM4 and BEAM44 elements for deck, 605 BEAM4 elements for the towers, 392 LINK11 elements for the cables, 64 LINK8 elements for the stabilizing cables, and 8 LINK8 elements for restraints of the bridge deck (The University of Hong Kong 2007). There are 5,610 nodes in total. The full bridge model is illustrated in Fig. 2.



Fig. 2 Full grid beam model of Ting Kau Bridge

All DOFs are assumed to be fixed at the base of each tower. The end girders at both the Ting Kau (TK) Pier and Tsing Yi (TY) Abutment are supported by rocker bearings that allow translational and rotational movements in the longitudinal directions and no movements in the transverse direction. Therefore, the ends of the girders are assigned roller supports that permit longitudinal translation and rotation, but not transverse movement. The deck-tower bearings are simulated using link elements such that longitudinal movements of the bridge deck are restricted while allowing vertical movements and small rotation about the transverse axis.

3. Simulation of random vehicular loading

Measurements of the vehicular axle loads were obtained from the weigh-in-motion system of the Wind and Structural Health Monitoring System (WASHMS) installed on TKB. The vehicles using TKB include categories covering cars, public service vehicles, light goods vehicles, medium goods vehicles, rigid goods vehicles, articulated heavy goods vehicles, buses, coaches, etc. with different axle loads. The analysis of vehicular loading obtained by WASHMS in the year 2007 is described here. The measured axle numbers in 19 bins and 6 lanes on TKB as shown in Table 1 are analysed. It is observed that, while more vehicles have used the TK-bound slow lane compared to that for the

Table 1 Measured axle load counts for various lanes on Ting Kau Bridge in the year 2007

Weight range (t)	Ting Kau bound carriageway			Tsing Yi bound carriageway		
	Slow lane	Middle lane	Fast lane	Slow lane	Middle lane	Fast lane
1~2	2,592,006	3,199,833	1,061,238	859,381	3,723,927	2,074,015
2~3	1,434,110	1,244,642	151,563	1,160,794	1,135,689	166,016
3~4	1,588,511	1,044,987	40,412	1,030,539	680,711	50,389
4~5	1,972,072	1,265,193	20,755	1,067,894	538,584	13,724
5~6	1,496,664	758,440	7,307	1,392,658	588,748	4,006
6~7	884,792	350,500	5,075	1,716,891	375,566	1,421
7~8	609,221	268,179	4,877	925,947	169,961	1,087
8~9	484,595	216,605	4,293	549,471	113,945	1,132
9~10	343,246	141,288	2,435	451,030	97,666	687
10~11	212,201	73,615	648	333,465	80,866	183
11~12	131,084	20,920	222	218,092	56,560	41
12~13	82,304	4,513	124	120,713	16,252	20
13~14	44,652	1,600	52	65,392	7,576	8
14~15	19,972	525	27	30,104	3,957	0
15~16	7,900	133	13	16,835	1,969	0
16~17	3,162	23	6	9,010	1,063	0
17~18	1,309	1	1	4,128	716	0
18~19	554	0	1	1,849	394	0
>19	407	4	17	1,452	1,948	0
Total	11,908,762	8,591,001	1,299,066	9,955,645	7,596,098	2,312,729

TY-bound slow lane, those using the TY-bound slow lane consist of more heavy vehicles primarily because of those trucks heading for the Kwai Chung Container Terminal further south for off-loading. However upon comparison of axle load counts for the fast lanes, it is observed that the TY-bound fast lane has carried more vehicles. This distribution of vehicles among the lanes may be governed by the interchanges on both sides of the bridge.

If one can determine a random variable to model the vehicular loading, one can generate the random vehicular axle loads for study of the random vibration. Unfortunately, the vehicular loading often does not fall into any common distributions such as normal distribution, lognormal distribution, extreme value distribution, gamma distribution, Poisson distribution, Weibull distribution, etc. The procedures adopted in the present study to generate the random vehicular axle loads with unknown distribution are as follows.

- (a) Obtain the vehicular axle load data from the WASHMS.
- (b) The range of magnitude of axle load is divided into a number of bins, with the typical bin i defined by its lower limit X_i^l and upper limit X_i^u . Note that in general $X_{i-1}^u = X_i^l$. The bin size of axle load range in the present case is set as 1 t. The threshold for axle load is chosen as 1 t so that any value below it will be neglected. The axle loads are classified as falling into bin 1 to bin 19 according to the weight range they belong to, namely 1~2 t, 2~3 t, ..., 18~19 t and values above 19 t respectively.
- (c) Obtain the axle load number for each bin and the total axle load number for all bins.
- (d) Calculate the probability P_i and cumulative probability F_i of the axle load number for each bin i respectively as

$$P_i = \frac{\text{Axle load number for bin } i}{\text{Total axle load number}} \tag{2}$$

$$F_i = \sum_{j=1}^i P_j \tag{3}$$

- (e) For each bin, it is assumed that the random variable of axle load is a uniform distribution for simplicity.
- (f) By means of the probability P_i and cumulative probability F_i in (d) and the assumption of (e), one can generate the random values of vehicular axle loads. Two pseudo-random numbers u_1 and u_2 are generated based on uniform probability density function over a unit interval for determination of the bin range (i.e., bin i) and magnitude X of each axle load as follows

$$\text{Axle load} \in \text{bin } i \quad \text{if} \quad u_1 \in [F_{i-1}, F_i) \tag{4}$$

$$X = X_i^l + u_2(X_i^u - X_i^l) \tag{5}$$

The generation of random vehicular axle load is elaborated using the TK-bound slow lane as an example. Based on the axle load measurements for TK-bound slow lane in 2007, the probability P_i and cumulative probability F_i of axle load are calculated as shown in Table 2. For each random axle load, two pseudo-random numbers u_1 and u_2 are generated based on uniform probability density function over a unit interval, and they are used for determination of axle load range and the magnitude of axle load. For instance, if the first generated pseudo-random number u_1 lies between the cumulative probability of axle load range 8~9 t (i.e., $F_{i-1} = 0.928893$) and that of axle load range 9~10 t (i.e., $F_i = 0.957716$), then the random axle load should lie within the range 9~10 t or bin i

Table 2 Probability and cumulative probability of axle load for TK-bound slow lane in 2007

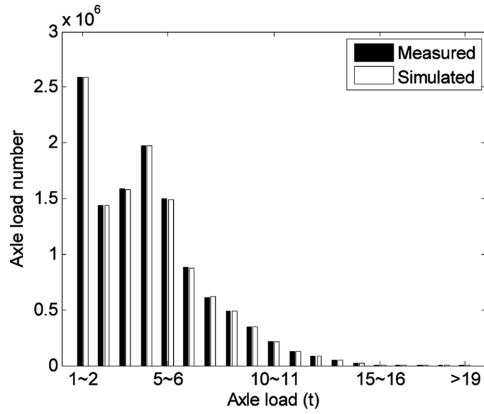
Weight range (t)	Axle load number	Probability	Cumulative probability
1~2	2,592,006	0.217655	0.217655
2~3	1,434,110	0.120425	0.338080
3~4	1,588,511	0.133390	0.471470
4~5	1,972,072	0.165598	0.637069
5~6	1,496,664	0.125678	0.762746
6~7	884,792	0.074298	0.837044
7~8	609,221	0.051157	0.888201
8~9	484,595	0.040692	0.928893
9~10	343,246	0.028823	0.957716
10~11	212,201	0.017819	0.975535
11~12	131,084	0.011007	0.986543
12~13	82,304	0.006911	0.993454
13~14	44,652	0.003750	0.997203
14~15	19,972	0.001677	0.998880
15~16	7,900	0.000663	0.999544
16~17	3,162	0.000266	0.999809
17~18	1,309	0.000110	0.999919
18~19	554	0.000047	0.999966
>19	407	0.000034	1.000000
Total	11,908,762		

($i = 9$). Again based on uniform probability density over the identified axle load range, the random axle load can be calculated as $9 + u_2 \times (10 - 9)$. The above steps can then be repeated to generate all random axle loads, which are assumed to be independent of one another.

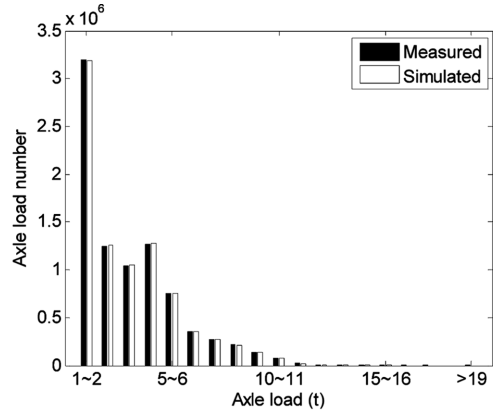
Using the above procedures, one can generate the random vehicular axle loads on the 3 TK-bound lanes and the 3 TY-bound lanes. To evaluate the performance of the above procedures, a chi-square goodness-of-fit test can be carried out between the random axle loads generated from step (f) and the measured axle loads. The statistic χ^2 for chi-square test is taken as

$$\chi^2 = \sum_{i=1}^N (S_i - M_i)^2 / M_i \quad (6)$$

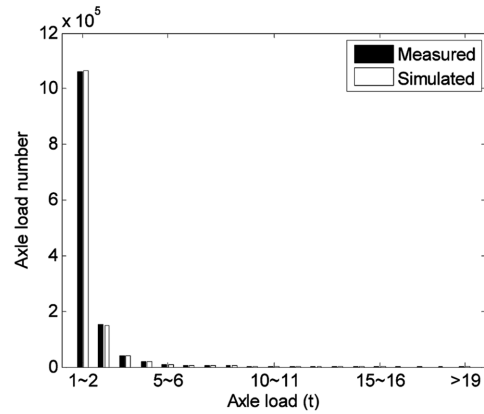
where S_i and M_i are the simulated and measured axle load counts in bin i , respectively, and N is the number of bins. The statistic has an approximate chi-square distribution when the counts are sufficiently large. If χ^2 calculated by Eq. (6) is less than $\chi^2_{0.05, N-1}$, the hypothesis that the simulated and measured axle loads have the same distribution cannot be rejected at the 5% significance level. Histograms of the measured and simulated axle loads on the 6 lanes are shown in Fig. 3 for comparison. Good agreement has been achieved between the measured and simulated axle loads on each lane, as confirmed by the chi-square goodness-of-fit test results shown in Table 3. Note that some values of N in Table 3 are less than 19 because of certain zero entries in Table 1. The values of $\chi^2_{0.05, N-1}$ in the rightmost column can be obtained from statistical textbooks such as that by Bickel and Doksum (2001). Therefore, one can use samples of simulated axle loads to study the random vibrations of TKB.



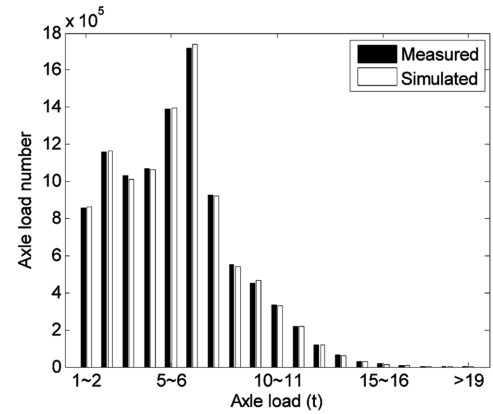
(a) Axle loads on TK-bound slow lane



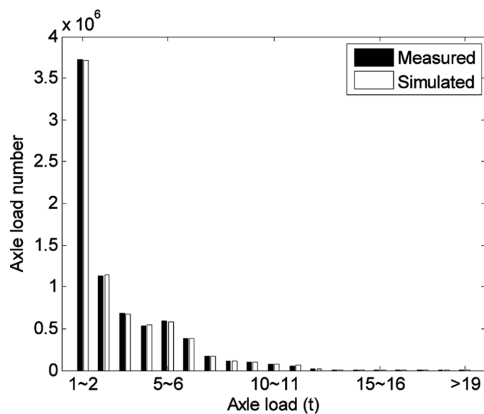
(b) Axle loads on TK-bound middle lane



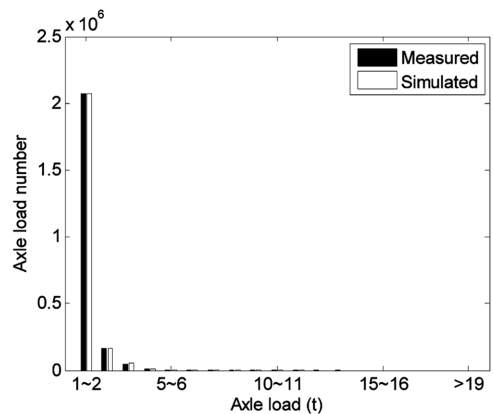
(c) Axle loads on TK-bound fast lane



(d) Axle loads on TY-bound slow lane



(e) Axle loads on TY-bound middle lane



(f) Axle loads on TY-bound fast lane

Fig. 3 Histograms of measured and simulation axle loads

Table 3 Results for chi-square goodness-of-fit test of the measured and simulated axle loads

Axle loads on different lanes	N	χ^2	$\chi^2_{0.05, N-1}$
TK-bound slow	19	10.92	28.87
TK-bound middle	18	14.62	27.59
TK-bound fast	19	15.27	28.87
TY-bound slow	19	16.33	28.87
TY-bound middle	19	10.82	28.87
TY-bound fast	13	16.47	21.03

4. General approach for dynamic analysis of TKB under moving axle loads

With the knowledge of assumed vehicle velocity and the time when the vehicular axle load first runs on the bridge, the position of vehicular axle load at any instant afterwards can be worked out. Because of the transverse spanning arrangement, a vehicular axle load acting on a carriageway of the bridge deck can be considered to exert two equivalent point loads on the two supporting main girders. When each of the point loads traverses a certain beam element of the main girder, the effects can be modelled by the time-varying forces and moments at the element nodes which constitute the consistent element load vector. The duration within which the axle loads travel on the bridge is divided into smaller time steps for solution as elaborated below. Then the dynamic analysis of the bridge under the moving vehicular axle loads can be carried out by time integration using the Newmark-beta method. The structure is assumed to have no damping. Results hereafter are those from dynamic analyses unless otherwise stated. Note that the assumed loading and solution strategy in the following sections may vary from case to case as elaborated there. In some cases, the dynamic responses are compared to static responses.

5. Dynamic responses of TKB under a moving determinate vehicular axle load along the first main girder

To get an idea of overall dynamic characteristics of TKB under moving loads, the dynamic responses of TKB under a hypothetical determinate 10 t vehicular axle load moving along the first main girder from Tsing Yi End to Ting Kau End at various velocities are studied. The duration within which the axle load travels on the bridge is divided into 1,000 equal time steps for solution by time integration. Fig. 4 shows the maximum vertical deflections of main girders at section A under the determinate axle load moving at various velocities. It can be seen that the maximum girder deflections increase slightly with the increase of velocity indicating mildly increasing contributions from dynamic responses. As expected, for the same velocity of moving axle load, the maximum vertical deflection decreases with increase of distance away from the loaded girder. In other words, it decreases in the order of the first, second, third and fourth main girders.

Fig. 5 shows the maximum vertical deflections of main girders at section B under the same loading. Similar to those at section A, the deflection also decreases with distance away from the loaded girder as expected. However the rising trend with velocity is less obvious because within the larger distance from the starting point to section B, more cancellations of responses have taken

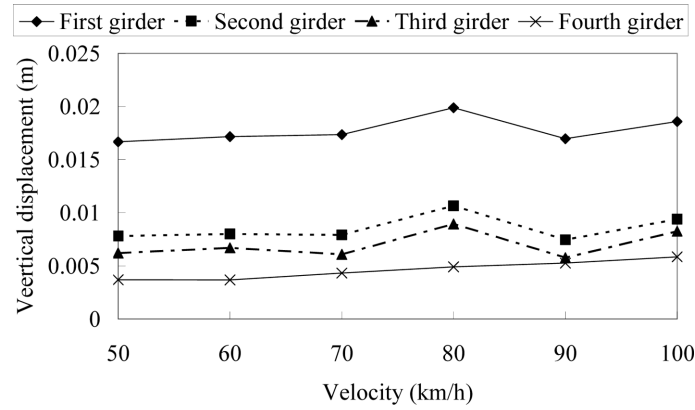


Fig. 4 Maximum vertical deflections of main girders at section A under a hypothetical axle load of 10 t moving along the first main girder at various velocities

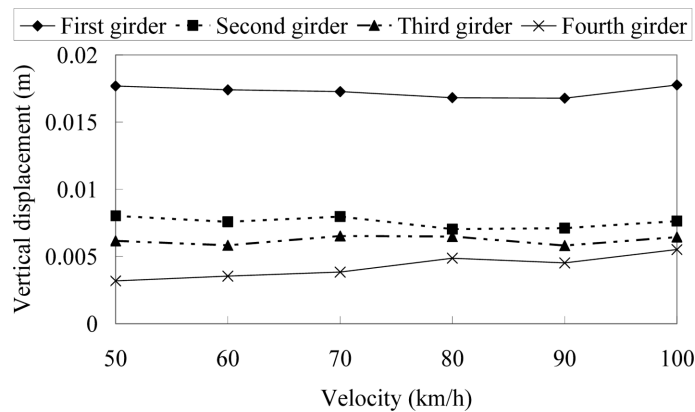


Fig. 5 Maximum vertical deflections of main girders at section B under a hypothetical axle load of 10 t moving along the first main girder at various velocities

place, whereas within the shorter distance to section A, the bridge is primarily in the excitation phase. Both Figs. 4 and 5 show that the maximum girder deflections are relatively insensitive to the velocity of moving axle load. In particular, no significant peaks associated with resonance are observed within this common velocity range.

6. Dynamic responses of TKB under moving random vehicular axle loads at uniform spacing on all traffic lanes

To investigate the dynamic responses of TKB under moving random vehicular axle loads, a hypothetical convoy of 50 random axle loads is generated for each of the 6 traffic lanes. The convoys in the lanes heading in each direction are considered to travel simultaneously along the bridge at the same velocity. Although the spacing between adjacent axles does vary, the axle spacing in the hypothetical convoy is assumed to be a typical value of 2.56 m in this section unless

otherwise stated. The effects of the other parameters will be examined later. TKB carries a total of 6 traffic lanes with 3 in each direction. Random loading in the form of convoys each comprising 50 random axle loads is generated by means of the procedure described in Section 3 based on the axle load measurements in the year 2007 for the 6 traffic lanes. As the carriageway widths vary slightly over certain lengths of the bridge adjacent to the interchange, a simplified method is adopted here to distribute the convoys of axle loads to the supporting main girders. For each carriageway, the random loading on the slow lane and half of that on the middle lane are assumed to act on the outer main girder, while the random loading on the fast lane and half of that on the middle lane are assumed to act on the interior main girder. Along the first and second main girders, the equivalent convoys move from Tsing Yi End to Ting Kau End, whereas the other equivalent convoys along the third and fourth main girders move from Ting Kau End to Tsing Yi End simultaneously at the same speed. The assumed speed at which the convoys move ranges from 50 km/h to 100 km/h. Similar to Section 5, the duration within which the convoys travel on the bridge is divided into 1,000 equal time steps for solution by time integration. Because of the random nature of the problem, the dynamic responses also depend on the vehicular axle loads generated. In view of the amount of computations necessary, for each velocity investigated, 4 random sample sets of convoys are used in the analysis for calculation of the statistics of dynamic responses of the bridge.

Fig. 6 shows the mean values of maximum vertical deflections of main girders at section A under random vehicular axle loads moving at various velocities on all lanes. It can be seen that the maximum vertical deflection of each main girder generally increases mildly with the increase of velocity of convoys. In addition, for the same velocity of convoys, the mean values of maximum vertical deflections of the outer main girders (i.e., first and fourth) are higher than those of the interior main girders (i.e., second and third). This is primarily caused by the higher proportion of heavy axle loads acting on the slow lanes adjacent to the outer main girders, which becomes obvious by comparing Figs. 3(a) and 3(d) with Figs. 3(c) and 3(f) respectively. For the same velocity, the mean values of maximum vertical deflections of the first and second main girders are less than those of the fourth and third main girders, respectively. It follows from the higher axle loads acting on the fourth main girder compared to that on the first main girder, which is obvious by reference to Table 1 or by comparing Fig. 3(a) with Fig. 3(d). The relatively large differences in

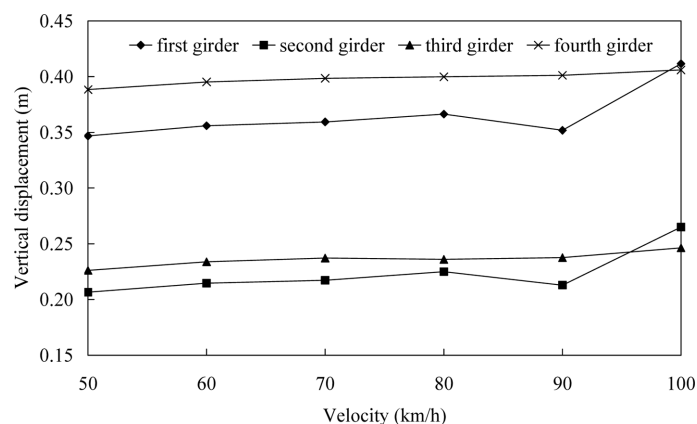


Fig. 6 Mean values of maximum vertical deflection of main girders at section A under random vehicular axle loads moving at various velocities on all lanes

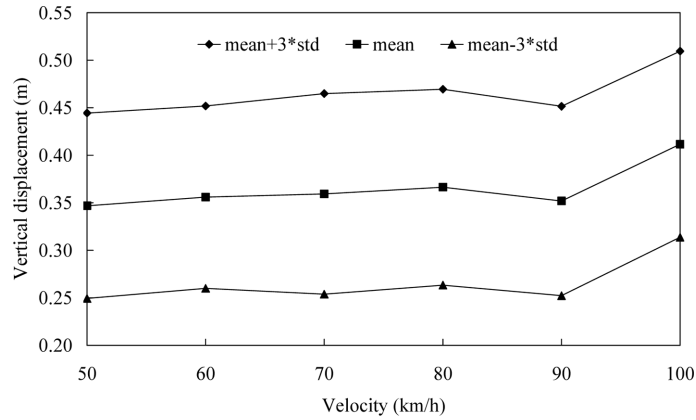


Fig. 7 Upper limit, mean value and lower limit of maximum vertical deflection of the first main girder at section A under random vehicular axle loads moving at various velocities on all lanes

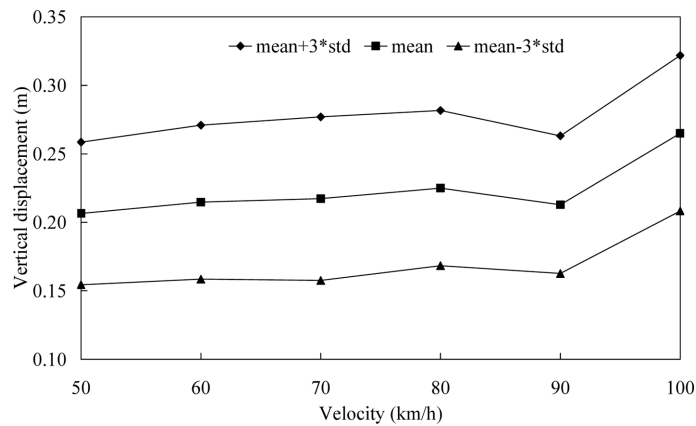


Fig. 8 Upper limit, mean value and lower limit of maximum vertical deflection of the second main girder at section A under random vehicular axle loads moving at various velocities on all lanes

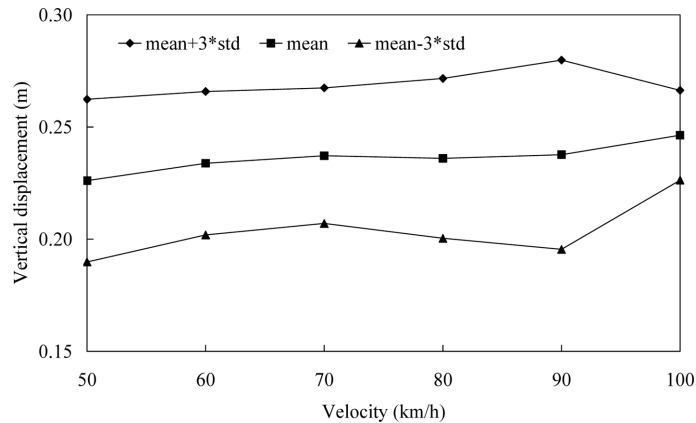


Fig. 9 Upper limit, mean value and lower limit of maximum vertical deflection of the third main girder at section A under random vehicular axle loads moving at various velocities on all lanes

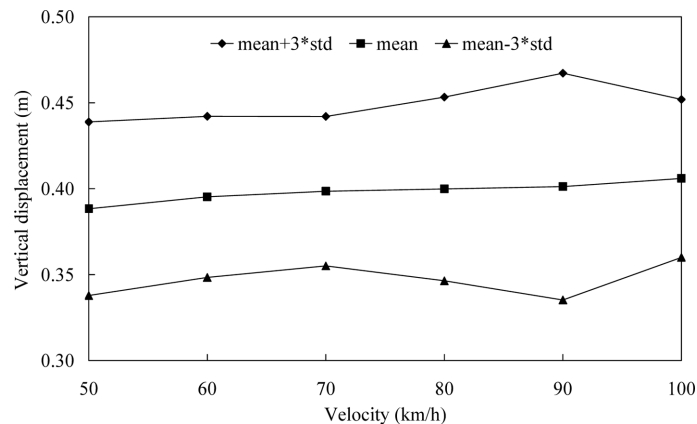


Fig. 10 Upper limit, mean value and lower limit of maximum vertical deflection of the fourth main girder at section A under random vehicular axle loads moving at various velocities on all lanes

vertical deflections between the outer and interior main girders also reflect to some extent the flexibility of the transverse girders of the deck.

To quantify the variations of the dynamic responses, the range of possible values is approximately defined by an upper limit arbitrarily taken as the mean value plus three times the standard deviation (std) and a lower limit arbitrarily taken as the mean value minus three times the standard deviation. Figs. 7-10 show the upper limits, mean values, and lower limits of maximum vertical deflection of the first, second, third and fourth main girders, respectively, at section A under random vehicular axle loads moving at various velocities on all lanes. In each of the cases examined, the upper limit and lower limit also tend to increase mildly with the increase of velocity of convoys, which is similar to the trend of mean value.

7. Factors affecting vehicular loading

The vehicular loading on a lane actually depends on a lot of factors, including the loading of each axle, number of axles and axle spacing in each vehicle, distances between vehicles in a lane, vehicle velocities, impact effects compared with the corresponding static load case, the number of vehicles in a convoy, etc. While it is acknowledged that the results depend on the chosen vehicle models (i.e., moving forces, moving masses and moving vehicles), the use of moving axle loads is the only practical means in view of the available weigh-in-motion measurements. The analyses in the previous section have been based on a convoy of 50 random vehicular axle loads on each of the traffic lanes generated based on the statistical models obtained from the measurements. Although such analyses have taken into account the transverse distribution of highway loading and random nature of axle load variations, the possible variations of axle spacing have not been taken into account. Instead of treating the axle spacing as yet another random variable in the present study, the implications of longitudinal distribution of axle loading are investigated by a deterministic approach in view of the substantial computations involved.

The axle load measurements captured by the weigh-in-motion system only provide information at the instant when each axle passes over it. Thereafter the arrangement of the axles as they run on the

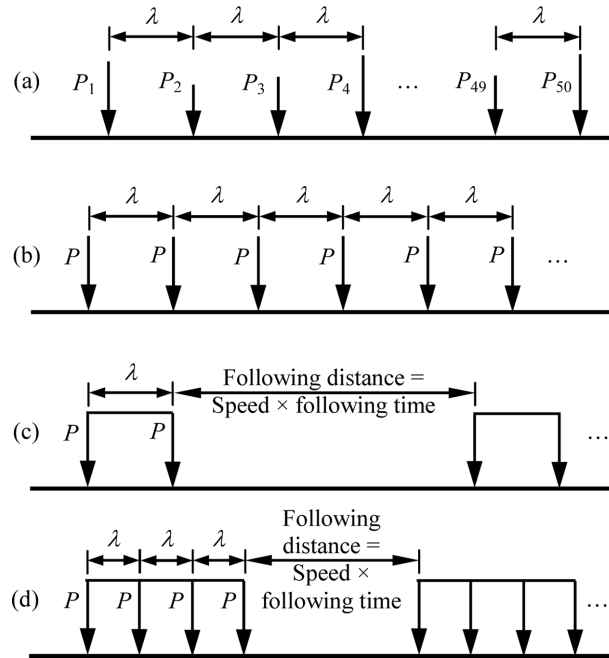


Fig. 11 Various hypothetical moving force models investigated (a) 50 axles of random or constant loading at constant spacing, (b) unlimited no. of axles of constant loading at constant spacing, (c) unlimited no. of identical 2-axle vehicles, and (d) unlimited no. of identical 4-axle vehicles

Table 4 Comparison of various hypothetical moving force models investigated

Model	Type of vehicles	Axle load	Number of vehicles	Spacing between vehicles
(a)	Single-axle	Random or constant (80 kN)	50	Constant
(b)	Single-axle	Constant (80 kN)	Unlimited	Constant
(c)	2-axle	Constant (80 kN)	Unlimited	Speed-dependent
(d)	4-axle	Constant (80 kN)	Unlimited	Speed-dependent

bridge may change. While the interior spacing between axles of a vehicle remains unchanged throughout, the distance between vehicles may change as their velocities may differ. In the present investigation of the effects of longitudinal arrangement of axle loads, various moving force models as shown in Fig. 11 and elaborated in Table 4 are applied only on the first main girder running at various velocities from Ting Kau to Tsing Yi. As the transverse distribution of axle loading has minimal effect on the maximum response due to overall behaviour of a long-span bridge, it is considered sufficient to examine the dynamic responses due to various hypothetical moving force models acting on one of the main girders only. Both static and dynamic analyses are carried out until the front axle reaches the other end of bridge. In particular, Model (a) with 50 random axle loads at constant spacing has been applied on various lanes in the analyses described in the previous section. For Model (a) with 50 constant axle loading and other models, each axle load is arbitrarily taken as 80 kN, which is in accordance with the standard fatigue vehicle in BS5400: Part 10 (British Standards Institution 1980). Model (a) with 50 constant axle loads is meant to provide

reference solutions for comparison with those obtained from Model (b) with unlimited number of axles. Models (c) and (d) simulate, respectively, 2-axle and 4-axle vehicles at constant spacing between vehicles. The axle spacing in Models (a) and (b) may appear unreasonably small for modelling the spacing between vehicles. There is the well-known “two-second rule” among considerate motorists to maintain a safe following distance with the vehicle in front. Although not every motorist observes this “two-second rule”, it is reasonable to take the distance between vehicles roughly as the velocity multiplied by a certain “following time” that may even be below 2 s. This assumption applies to all motorists except for a few irresponsible tailgating drivers. As the longitudinal arrangement of axle loads depends also on the velocity, even the static results are dependent on velocity.

Static and dynamic analyses are carried out for Model (a) with 50 constant axle loads and Model (b) with unlimited axles at various constant spacing all moving at 50 km/h on the first main girder. The deterministic approach adopted here allows a more sophisticated scheme for time integration. The consistent load vector to account for the moving axle loads is updated at intervals corresponding to the movement by 0.1 of the length of a typical beam element to model the main girder. The time step for dynamic analysis is taken to correspond to the movement by 0.001 of the length of a typical beam element. As there are 449 beam elements in each main girder, the total number of time steps for time integration here is much higher than that in the previous sections. For convenience in comparison, the axle loading is expressed in terms of an equivalent uniformly distributed loading taking into account the size of vehicle and spacing between vehicles. The maximum vertical displacements of the first main girder at section A as an indicative response are shown in Fig. 12. In general, a lower axle spacing with a higher equivalent uniformly distributed load normally gives rise to a higher maximum response. The rate of increase of maximum response with equivalent uniformly distributed load is higher for cases with unlimited axles. The higher maximum dynamic response compared to that of the static response accounts for the impact effect. The impact effect varies from case to case but does not exceed 32%. As the structural model is

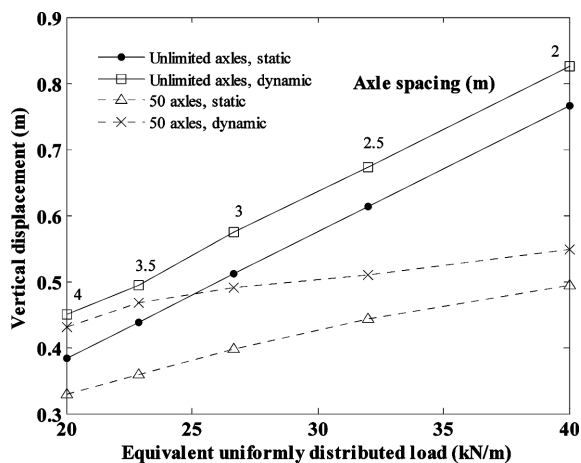


Fig. 12 Maximum vertical deflection of the first main girder at section A under Model (a) with 50 constant axles and Model (b) with unlimited number of axles moving at 50 km/h on the first main girder

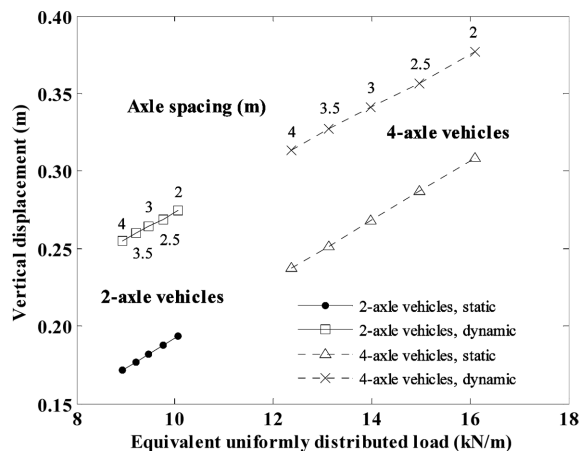


Fig. 13 Maximum vertical deflection of the first main girder at section A under Models (c) and (d) with various interior axle spacing moving on the first main girder at 50 km/h and following time of 1 s

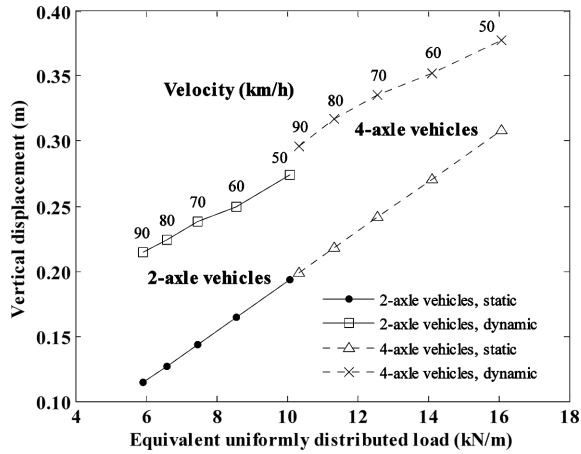


Fig. 14 Maximum vertical deflection of the first main girder at section A under Models (c) and (d) with interior axle spacing of 2 m moving on the first main girder at various velocities and following time of 1 s

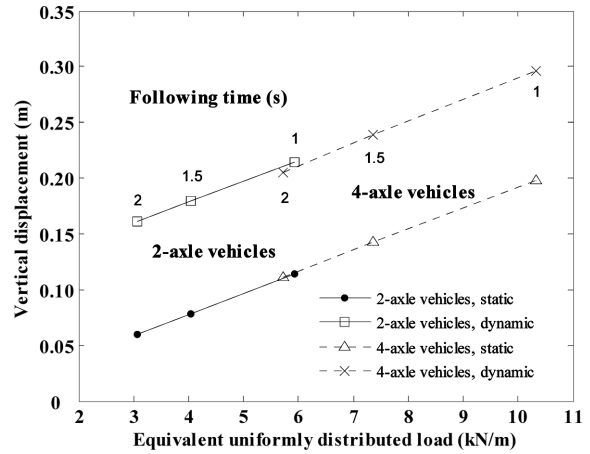


Fig. 15 Maximum vertical deflection of the first main girder at section A under Models (c) and (d) with interior axle spacing of 2 m moving on the first main girder at velocity of 90 km/h and various following time

assumed to have no damping, these calculated impact effects are conservative estimates.

The effects of modelling highway loading by multi-axle vehicles at realistic inter-vehicle spacing are then investigated. The static and dynamic responses of the bridge under 2-axle vehicles, i.e., Model (c), and 4-axle vehicles, i.e., Model (d), with various interior axle spacing moving on the first main girder at 50 km/h and following time of 1s are obtained. Fig. 13 shows the maximum vertical displacements of the first main girder at section A plotted against the equivalent uniformly distributed load. The maximum responses gradually increase with equivalent uniformly distributed load for each type of vehicles. In particular, the static results of both types of vehicle virtually lie on the same straight line. The same trend also applies to the dynamic results approximately.

To investigate the effects of realistic inter-vehicle spacing, the static and dynamic responses of the bridge under 2-axle vehicles and 4-axle vehicles with interior axle spacing of 2 m are worked out. The maximum vertical displacements of the first main girder at section A for hypothetical vehicles moving on the first main girder at various velocities and following time of 1s are plotted in Fig. 14. For each type of vehicles, the inter-vehicle spacing at a fixed following time increases with velocity thereby resulting in a reduced equivalent uniformly distributed load. A general trend of increasing response with increasing equivalent uniformly distributed load is noted. While the static results of both types of vehicle again fit nicely into the same straight line, the dynamic results have shown more deviation from the common trend line. Fig. 15 shows the corresponding responses for hypothetical vehicles moving on the first main girder at 90 km/h and various values of following time. Note that a longer following time increases the inter-vehicle spacing thereby reducing the equivalent uniformly distributed load. A similar trend between the responses and the equivalent uniformly distributed load is noted.

It is noted from the above studies that the effects of the number of axles and axle spacing within vehicles and the inter-vehicle spacing are different. The above factors have to be considered in further work on random generation of highway loading models based on weigh-in-motion measurements.

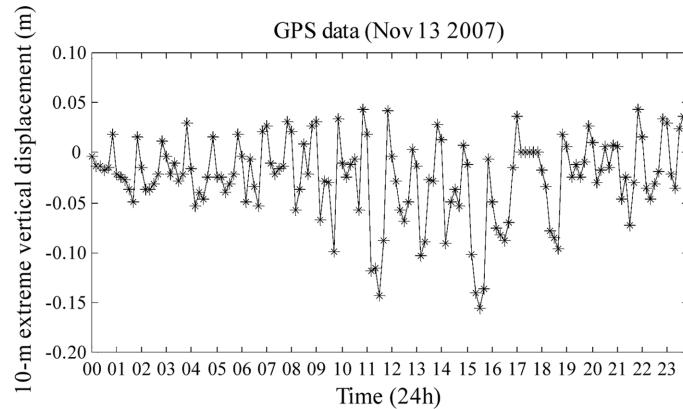


Fig. 16 Diurnal variation of deck vertical displacement of the first main girder at section A on 13 November 2007 (positive value denotes upward displacement)

8. Comparison with field measurements

In order to assess how well the finite element model predicts the bridge responses due to vehicular loading, the GPS data at section A for a typical day as obtained from the WASHMS are therefore analysed for comparison. Fig. 16 shows the extreme vertical displacements of the first main girder at section A on 13 November 2007 calculated over 10-minute periods, in which a positive value denotes upward displacement. The extreme displacements are observed to occur before and after lunch time, with the maximum downward displacement of 0.156 m occurring at 3:30 pm.

As there are many factors affecting the actual loading on the bridge and therefore the resulting numerical predictions, only a rough comparison is attempted here. Fig. 7 shows that over the velocity range of 50 km/h to 90 km/h, the maximum vertical displacements of the first main girder at section A due to 50 random vehicular axle loads at constant axle spacing of 2.56 m generated based on the identified statistical model lie roughly between 0.25 m and 0.45 m. Results from Figs. 12 and 14 due to series of 80 kN axle loads may be used for rough conversion of the calculated maximum vertical displacements of the first main girder at section A to realistic situations. Fig. 12 shows the maximum vertical displacement for 50 axles at constant axle spacing of 2.5 m considering dynamic effects to be around 0.51 m. Fig. 14 gives the maximum vertical displacement for 2-axle vehicles moving at 70 km/h with a following time of 1 s considering dynamic effects to be around 0.24 m. Note that although the “two-second rule” is advocated by the Government, a smaller value of following time is often observed on the roads. Therefore conversion from the 50 axles at constant axle spacing of 2.5 m to 2-axle vehicles with common following time involves a reduction factor of around $0.24 \text{ m} / 0.51 \text{ m} = 0.47$. Applying this reduction factor of 0.47 to the limits of 0.25 m and 0.45 m from Fig. 7 gives more realistic limits of 0.12 m and 0.21 m. The maximum downward displacement of 0.156 m in Fig. 16 is observed to lie within such limits. The assumption of no damping is a likely reason why the predicted displacements are slightly on the high side.

9. Conclusions

From the present work, the following observations can be made:

- (a) A procedure to simulate the random vehicular axle loads based on the measurements obtained from weigh-in-motion systems has been developed. It enables random axle loads to be generated such that their statistics agree broadly with the field measurements. This not only enables realistic dynamic analysis to be carried out but it will also be useful to the development and updating of reliability-based bridge design codes.
- (b) From the present study of Ting Kau Bridge, the maximum vertical deflections of the main girders under vehicular axle loads tend to increase mildly with the increase of velocity of the vehicles.
- (c) The differences among vertical deflections of various main girders reflect not only the transverse flexibility of the deck but also the transverse distribution of vehicular traffic on the bridge.
- (d) The variations of dynamic response tend to be higher at the main girders primarily carrying the slow lanes.
- (e) The number of axles and axle spacing within vehicles and the inter-vehicle spacing are identified to be essential factors for further work on random generation of highway loading models based on weigh-in-motion measurements. Good correlation is observed between the maximum responses and the equivalent uniformly distributed load resulting from the axle loading.
- (f) The observed displacements are comparable to the predicted results with suitable corrections to account for limitations of the present model.

Acknowledgements

The authors are grateful to the Highways Department of the Hong Kong Government for permission to publish this paper. Any opinions expressed or conclusions reached in the paper are entirely of the authors.

References

- Au, F.T.K., Jiang, R.J., Leung, C.C.Y., Xie, L.Z., Lee, P.K.K., Wong, K.Y. and Chan, W.Y. (2007), "Development and calibration of finite element models for structural health monitoring of Ting Kau Bridge", Invited Lecture, *Proceedings of International Symposium on Environmental Vibrations (ISEV 2007)*, Taipei, Taiwan, November.
- Au, F.T.K., Tham, L.G., Lee, P.K.K., Su, C., Han, D.J., Yan, Q.S. and Wong, K.Y. (2003), "Ambient vibration measurements and finite element modelling for the Hong Kong Ting Kau Bridge", *Struct. Eng. Mech.*, **15**(1), 115-134.
- Au, F.T.K., Wang, J.J. and Cheung, Y.K. (2002), "Impact study of cable-stayed railway bridges with random rail irregularities", *Eng. Struct.*, **24**(5), 529-541.
- Bickel, P.J. and Doksum, K.A. (2001), *Mathematical Statistics: Basic Ideas and Selected Topics*, Vol. 1, 2nd Edition, Prentice-Hall Inc., New Jersey.
- British Standards Institution (1980), *BS5400: Part 10, Steel, Concrete and Composite Bridges – Code of Practice for Fatigue*, London.
- Chang, T.P., Liu, M.F. and O, H.W. (2009), "Vibration analysis of a uniform beam traversed by a moving vehicle

- with random mass and random velocity”, *Struct. Eng. Mech.*, **31**(6), 737-749.
- Coussy, O., Said, M. and Vanhoove, J.P. (1989), “The influence of random surface irregularities on the dynamic response of bridges under suspended moving loads”, *J. Sound Vib.*, **130**(2), 313-320.
- Jo, J.S., Jung, H.J. and Kim, H. (2008), “Finite element analysis of vehicle-bridge interaction by an iterative method”, *Struct. Eng. Mech.*, **30**(2), 165-176.
- Law, S.S. and Zhu, X.Q. (2005), “Bridge dynamic responses due to road surface roughness and braking of vehicle”, *J. Sound Vib.*, **282**(3-5), 805-830.
- Lee, C.H., Kawatani, M., Kim, C.W., Nishimura, N. and Kobayashi, Y. (2006), “Dynamic response of a monorail steel bridge under a moving train”, *J. Sound Vib.*, **294**(3), 562-579.
- Li, Q., Xu, Y.L., Wu, D.J. and Chen, Z.W. (2010), “Computer-aided nonlinear vehicle-bridge interaction analysis”, *J. Vib. Control*, **16**(12), 1791-1816.
- Kawatani, M., Kobayashi, Y. and Takamori, K. (1998), “Non-stationary random analysis with coupling vibration of bending and torsion of simple girder-bridge under moving vehicles”, *Struct. Eng. Earthq. Eng.*, **15**(1), 107-114.
- Kwasniewski, L. and Li, H.Y. (2006), “Finite element analysis of vehicle-bridge interaction”, *Finite Elem. Anal. Des.*, **42**(11), 950-959.
- Song, M.K. and Choi, C.K. (2002), “Analysis of high-speed vehicle-bridge interactions by a simplified 3-D model”, *Struct. Eng. Mech.*, **13**(5), 505-532.
- Song, M.K. and Fujino, Y. (2008), “Dynamic analysis of guideway structures by considering ultra high-speed Maglev train-guideway interaction”, *Struct. Eng. Mech.*, **29**(4), 355-380.
- The University of Hong Kong (2000), *Ting Kau Bridge: Ambient Vibration Measurement of Complete Bridge*, Report Prepared for the Bridges and Structures Division, Highways Department, Government of the Hong Kong Special Administrative Region.
- The University of Hong Kong (2007), *Ting Kau Bridge: 3D Finite Element Grid Beam Model of the Global Bridge Structure*, Report Prepared for the Bridges and Structures Division, Highways Department, Government of the Hong Kong Special Administrative Region.
- Wang, T.L. and Huang, D.Z. (1992), “Cable-stayed bridge vibration due to road surface roughness”, *J. Struct. Eng.-ASCE*, **118**(5), 1354-1373.
- Wiriyachai, A., Chu, K.H. and Garg, V.K. (1982), “Bridge impact due to wheel and track irregularities”, *J. Eng. Mech.-ASCE*, **108**(4), 648-666.
- Wu, Y.S. and Yang, Y.B. (2003), “Steady-state response and riding comfort of trains moving over a series of simply supported bridges”, *Eng. Struct.*, **25**(2), 251-265.
- Yang, Y.M., Pan, J.Y. and Cheng, Q.G. (1995), “Theoretical and experimental studies of the dynamic response of long span railway bridge (in Chinese)”, *China Railway Science*, **16**(4), 1-15.
- Yang, Y.B. and Lin, C.W. (2005), “Vehicle bridge interaction dynamics and potential applications”, *J. Sound Vib.*, **284**(1-2), 205-226.